Journal of the European Ceramic Society 16 (1996) 893–898

0955-2219(95)00208-1
0955-2219/96/$15.00 +.00

Study of the Behaviour of Aluminium Nitride in the Iron and Steel Industry

J. C. Labbe & A. Laïmeche

Laboratoire de Matériaux Céramiques et Traitements de Surface (CNRS URA 320), Université de Limoges, 123 av. Albert Thomas, 87060 Limoges Cedex, France

(Received 12 September 1994; revised version received 14 November 1995; accepted 29 November 1995)

Abstract

Reactivity studies of different steels with nitride ceramics, and in particular with aluminium nitride, have shown the presence of complex chemical reactions at the solid–liquid and liquid–vapour interfaces. Reaction at the AlN–liquid steel interface shows a decomposition of AlN followed by the oxidation of aluminium, and an AlON phase attack at grain boundaries.

L'étude de la réactivité de différentes nuances d'acier sur les céramiques nitrures et en particulier sur le nitrure d'aluminium, a mis en évidence l'existence d'interactions chimiques complexes aux interfaces liquide–vapeur et solide–liquide. L'interaction à l'interface AlN-acier liquide fait appel d'une part à un mécanisme de décomposition d'AlN avec oxydation de l'aluminium, et d'autre part à l'attaque de la phase AlON aux joints de grains de AlN.

Introduction

The continuous casting of steel presents many advantages, such as economy of energy and best use of raw materials. However, some drawbacks can be found, in particular corrosion of the refractory materials used in foundries, which limits the productivity of installations and affects the steel quality. For these reasons, specialists now are looking toward nitride ceramics and particularly aluminium nitride, which theoretically has good thermochemical stability and low solubility in liquid steel at high temperature (Table 1).

In the present work we are interested in the behaviour of pure AlN in contact with three types of steel: steel A (extra-mild low carbon), steel B (SiCa treated) and steel C (IFS ultra-low carbon). The corrosion problem will be considered in terms of the wettability of AlN surfaces by liquid steels and subsequent interaction as a function of time, temperature and surface porosity.

Theoretical Approach

Solid or liquid reactions can be explained by the surface phenomena of contact angle and surface tension, and by the physicochemical characterization of the intermediate reaction zone.

The simplified fundamental relation [eqn (1)] of Young and Dupre[2] links the contact angle θ to the three surface tensions, σ_{SV}, σ_{SL} and σ_{LV}, of the solid–vapour, solid–liquid and liquid–vapour interfaces, respectively:

$$\sigma_{SV} = \sigma_{SL} + \sigma_{LV}\cos\theta \quad (1)$$

so

$$\cos\theta = (\sigma_{SV} - \sigma_{SL})/\sigma_{LV} \quad (2)$$

σ_{LV} being positive, it is possible to determine the degree of wettability from eqn (2).[3]

$$(\sigma_{SV} - \sigma_{SL}) > 0 \quad \theta < 90°$$
$$(\sigma_{SV} - \sigma_{SL}) < 0 \quad \theta > 90°$$

These mechanical considerations suppose the existence of a solid–liquid interface which can only be possible by thermodynamic considerations when the system is under chemical equilibrium.[4,5] The surface tensions and also the degree of wettability depend on the nature of the reactions at the surfaces. A correlation between the degree of wettability and the presence of a chemical reaction at the interface seems to be possible (Fig. 1) and is accepted by many authors.[6]

Experimental Methods

Wettability apparatus

The equipment employed for the sessile drop method uses an analysis apparatus composed of a furnace, an optical system and a camera coupled with a computer. More details can be found elsewhere.[8]

Table 1. Solubility of some ceramics in liquid iron at 1600°C

Ceramic	*Solubility (mol l^{-1})*
AlN	0·21
BN	0·45
Si_3N_4	1·29
Al_2O_3	$1·02 \times 10^{-3}$
SiO_2	0·018

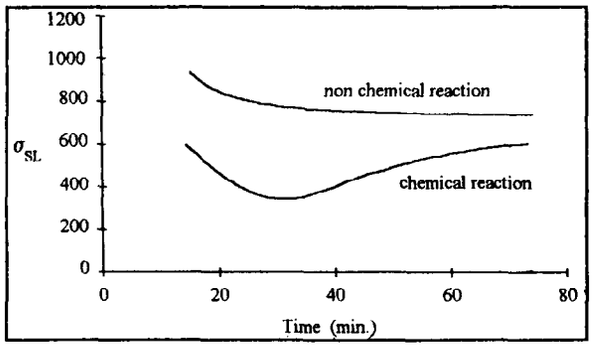

Fig. 1. Evolution of σ_{SL} as a function of time.[6,7]

Finger dipping method

This method consists of dipping AlN samples into different liquid steel baths. Molten steels are contained in small alumina moulds, which could be considered as a small-scale reproduction of the conditions existing in industry.

Materials used

The AlN powder used was produced by H. C. Starck (Berlin) and contains 1·4% oxygen, 33·1% nitrogen and 64·5% aluminium.

We prepared samples of cylindrical form with 35 mm diameter and 4 mm thickness, so that about 12 g of powder was required for each sample. Densification and operating conditions are given in Table 2. The densification of AlN has been studied by Ado *et al.*,[9] who showed that at high temperature (above 1600°C) the formation of AlON phase at grain boundaries is inevitable. This amorphous phase is useful for densification during sintering due to its high diffusion rate. At low temperature (below 1600°C) the AlON phase does not form during sintering. Its absence gives pure sintered material but is detrimental for good densification (see Table 2).

The steel samples employed had a cylindrical form with 6 mm diameter. Their compositions are given in Table 3. Their melting points are 1528, 1515 and 1532°C, respectively.

Table 2. Sintering conditions of pure AlN

P(MPa)	23	18·7	18·7
Temperature (°C)	1820	1600	1550
Time (min)	30	15	20
d_a/d_{th} (%)	97·3	84	78

Table 3. Steel compostion in ppm (major)

	Steel		
	A	*B*	*C*
C	430	1000	60
Si	120	3430	50
Al	450	250	440
Ti	0	110	670
N	46	36	26
Mn	1940	13730	1850

Experimental procedure

Metallic samples were placed on the ceramic substrate in the middle of the furnace in the sight of the camera. The system was kept under vacuum until a temperature of 1490°C was attained, after which argon was introduced in the furnace with a slight gauge pressure. The system was then brought to the working temperature at a rate of 30°C min^{-1}.

For the finger dipping method, small AlN bars with variable density (97·3, 90 and 84%, respectively) were dipped into liquid steels bath for 1 h, under 1 bar pressure of argon (introduced at low temperature), and at temperatures of 1550, 1600 and 1650°C.

Experimental Results

Contact angle

Contact angle is reduced when the temperature increases (Fig. 2) and finally stabilizes above 1580°C at $\theta < 90°$ for steel B and at $\theta > 90°$ for steels C and A; the latter were found to swell between temperatures of 1580 and 1620°C which can be attributed to the formation of gas at the interface.

At constant temperature the wetting angle decreases rapidly during the first 15 minutes (Fig. 3) and then stabilizes at a wetting angle ($\theta < 90°$) for steels A and B and at a non-wetting angle ($\theta > 90°$) for steel C at all temperatures, 1550 or 1570°C.

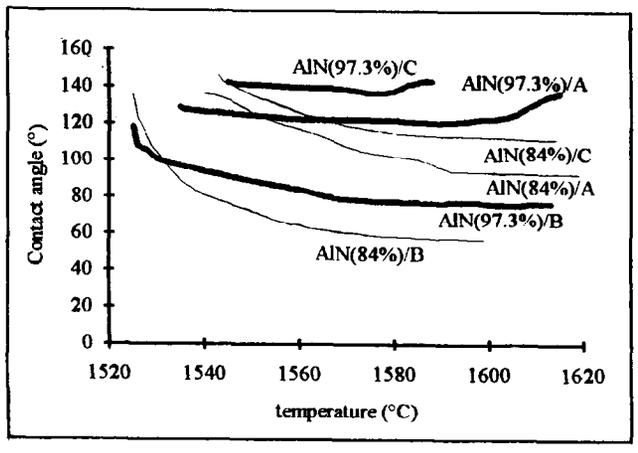

Fig. 2. Contact angle evolution of steel/AlN with temperature.

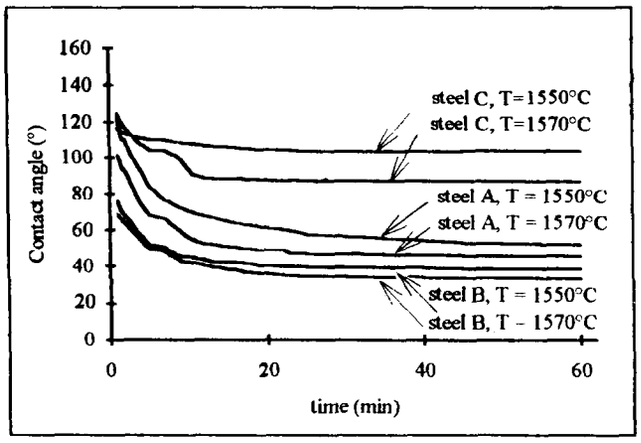

Fig. 3. Contact angle evolution of steel/AlN dense (d/d_{th} = 97·3%).

An increase in porosity decreases the wetting angle considerably, as can be shown by considering the slope $d\theta/dT$ calculated (Fig. 2) after 10 min of heating. For steel A/AlN, the slope varies from –0·1 to –0·85 for temperatures between 1540 and 1580°C, when the ceramic density decreases from 97·3 to 84%. We note that these results are in contradiction with those of Wenzel[10] and Rhee.[11] This can be explained through the fact that an important value of open porosity cannot be assimilated by surface rugosity and that this porosity has altogether different effects.

The effect of atmosphere was studied using the following two conditions:

(1) after having obtained a secondary vacuum of about 5×10^{-2} Pa, argon was introduced at T = 200°C. Argon pressure was kept at $1{\cdot}1 \times 10^5$ Pa;

(2) The furnace was kept under vacuum (6×10^{-2} Pa) up to a temperature of 1490°C and argon gas was introduced into the furnace at this temperature.

In the first case, the wetting angle remains practically constant and non-wetting (Fig. 4) at 1570°C while, in the second case, the angle reduces rapidly to $\theta < 90°$. This different behaviour is due to the presence of a solid layer on the liquid surface, observed just after fusion in the first case and after ~ 40 to 50 min in the second case. This layer probably arises from a reaction between the liquid surface and the impurities present in the atmosphere such as oxygen, prohibiting a normal contact angle evolution. In the case of steel C, this layer makes difficult the formation of a liquid drop.

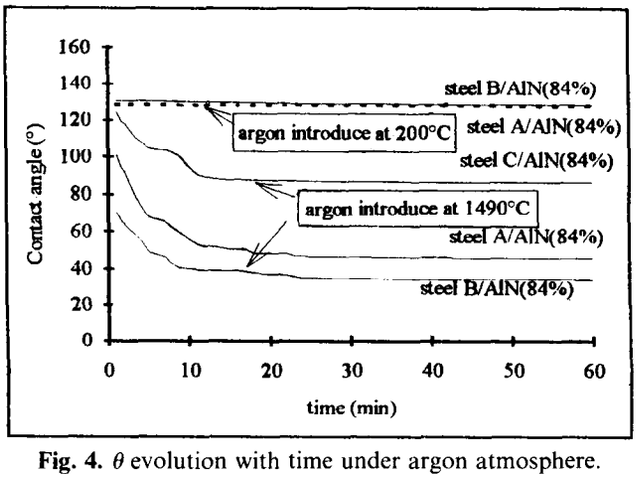

Fig. 4. θ evolution with time under argon atmosphere.

Solid–liquid tension

It is clear that the evolution of the liquid–vapour tension (σ_{LV}) cannot give a complete explanation of the wettability evolution.[12] Therefore, to understand liquid steel behaviour on solid substrates, it is necessary to follow the variation of σ_{SL} as a function of different parameters. A direct measurement of solid–liquid surface tension being impossible, we can only approach its value and its variation using the Young–Dupre equation (1). As done by a number of authors,[13,14] we can give a fixed value to σ_{SV} (1000 mN m^{-1}), θ and σ_{LV} being known through direct measurement or calculation. After that we can only consider the evolution σ_{SL} with respect to different parameters and not its absolute value.

It must be noted that the Young–Dupre equation can only be applied to systems that are in perfect mechanical and thermodynamical equilibrium and to surfaces that are perfectly plane, having very little rugosity. These conditions generally do not prevail during experiments. Thus σ_{SL} values obtained are approximate to a certain extent, but as we are more interested in the evolution of this value rather than its absolute value, we can admit such approximations.

The solid–liquid tension for steels A, B and C over aluminium nitride decreases just after the melting point of the steels (Fig. 5). Generally, high values of σ_{SL} show the presence of a chemical reaction at the interface.[6] At a constant temperature, the solid–liquid tension reaches a minimum value, in each case after 10 min, and becomes stable afterwards (Fig. 6). Experimental curves are

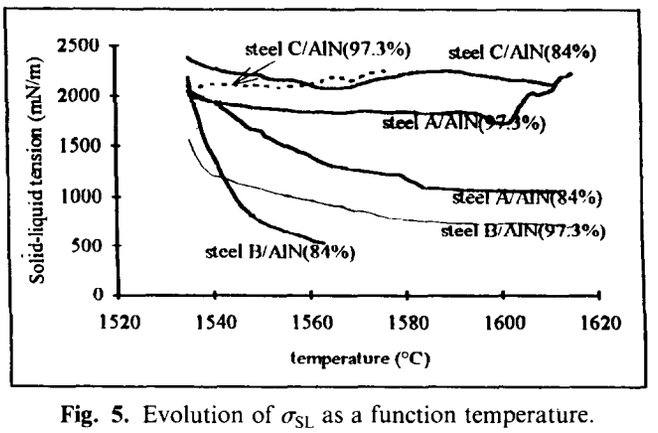

Fig. 5. Evolution of σ_{SL} as a function temperature.

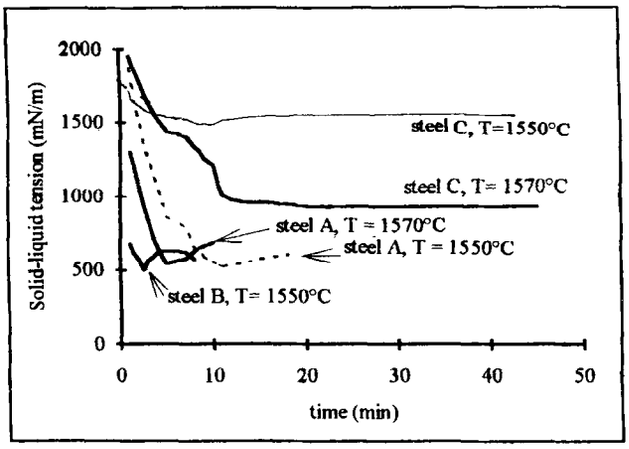

Fig. 6. σ_{SL} evolution of steel/AlN dense (d/d_{th} - 97·3%).

Table 4. The corrosion thickness (mm) of AlN in liquid steels (1 h; 1·1 × 10^5 Pa)

Steel	d/d_{th} (%)					
	97·3		*90*		*84*	
	1550°C	*1650°C*	*1550°C*	*1650°C*	*1550°C*	*1650°C*
A	–	–	0·03	0·65	0	0·1
B	0·22	0·28	0·27	0·2	0	0·06
C	0·16	>0·8	0·8	0·48	0	0·16

characteristic of a chemical reaction at the interface (see Fig. 1).

Porosity has an important influence on the solid–liquid tension (see Fig. 5) and σ_{SL} decreases when the porosity increases. Such behaviour can be explained if we consider that this phenomenon takes place in parallel with the chemical reaction at the interface. While porosity increases, the reaction at the surface gives a higher value of the variation $\Delta\sigma_{SL}$ of σ_{SL}, which is still enhanced by the wetting behaviour of steels A and B.

Results with the finger dipping method confirm these observations and show that higher corrosion values are obtained when the porosity is below 10%. An increase of the corrosion resistance is found when the porosity is around 20% (Table 4).

Discussion and Interpretation of Results

The decrease in θ value during the first 15 min after drop formation at constant temperature, characterizes a system that is out of chemical equilibrium. This behaviour was found at each temperature investigated. It should be noted that a higher porosity (>10%) rapidly decreased the contact angle to a very small value (see Fig. 2). These observations help us to conclude that the wetting angle is controlled by chemical reaction at the liquid steel–AlN interface. The variation of the solid–liquid interfacial tension as a function of time (Fig. 6) passed through a minimum value, for all types of steel. Such an evolution is further evidence for the presence of a chemical reaction at the interface.[6]

Observations made during the experiments —such as the swelling of the liquid drop and the bursting of these drops promoted by gas formation and elimination, and the formation of a solid layer at the liquid drop surface — show the presence of two chemical reactions: one at the solid–liquid interface and the other at the liquid–vapour interface. These will be discussed in the following sections.

Chemical interaction at solid–liquid interface

Scanning electron microscopy (SEM) and energy dispersive analysis by X-rays (EDAX) show that the liquid steel penetrates into the solid surface and also the presence of grains ($r \leq 5$ μm) distributed in the liquid phase. EDAX of these grains reveals a high concentration of Al and O and a very low concentration of N. We can postulate that this oxide is produced by a chemical reaction between AlN or AlON present at grain boundaries and the oxygen dissolved in the liquid steel or present in the nitride as impurities. Both reactions can take place simultaneously.

(1) Oxidation of nitride by oxygen dissolved in the liquid steel. The reaction take place in two stages, decomposition of nitride into Al and N, and oxidation of liquid Al:

$$AlN_{(sol)} \rightarrow [Al_{(liq)}]_{steel} + \frac{1}{2} N_2 \uparrow$$

$$\Delta G_R = -0{\cdot}17 + 7{\cdot}6\ \ln[P_{(N_2)}] = -28{\cdot}47\ \text{kJ mol}^{-1}$$

when T = 1820 K and $P_{N_2} = 10^{-7}$ atm

$$2[Al_{(liq)}]_{steel} + 3[O]_{steel} \rightarrow Al_2O_{3(sol)}$$

$$\Delta G^0_R = -498{\cdot}41\ \text{kJ mol}^{-1} \text{ at } 1820\ \text{K}$$

(2) Oxygen attack over AlON present at grain boundaries of sintered AlN, according to the following reactions:

$$2AlON_{(sol)} + [O]_{(steel)} \rightarrow Al_2O_{3(sol)} + N_{2(gas)} \uparrow$$

$$Al_2O_{3(sol)} \xrightarrow{\text{(steel)}} [Al_2O_3]_{(steel)}$$

All reactions lead to the formation of Al_2O_3. Theoretically, the steels used are saturated in alumina. The dissolution is probably not possible and we can suggest that Al_2O_3 remains at the interface, and the system advances towards a steel–Al_2O_3 contact. Thus it would be interesting to make some experiments to verify the reaction between steel and Al_2O_3. A study of the behaviour of pure and densified alumina with respect to steels A, B, and C shows[15] that the wetting angle and solid–

liquid tension (Figs 7 and 8) remain practically constant as a function of time. An alumina sample dipped into liquid steel at 1600°C for 10 h does not show any corrosion marks.

In the case of the reaction between steel and AlN, the main difference lies in the fact that the Al_2O_3 phase does not form a protective layer at the AlN surface. Thus a small amount of this alumina is possibly found in the liquid steel drop. The X-ray analysis does not allow us to detect this phase and we can imagine that it is an amorphous form of Al_2O_3. The results of the dipping experiment prove that the attack on the AlON phase present at the grain boundaries is the principal mechanism of corrosion by steels, and when the sintering conditions prevent the formation of AlON phase (temperature <1600°C), the corrosion decreases in a very important way. Thus, a high porosity sample sintered at low temperature presents the best resistance to corrosion (Table 4) in spite of the increase in the contact surface between the steel and the substrate due to the presence of pores.

In addition to AlON reaction, thermodynamic calculations confirm that AlN in all cases reacts with the oxygen present as traces in the furnace atmosphere.[16] This explains the mechanism of corrosion which results in gas (N_2) formation inside the liquid drop and its bursting. If we consider the works of Billy *et al.*[17] and Darbha[18] related to aluminium nitride corrosion, we note that the reaction at the interface resulting in nitrogen formation produces porosity at the interface. This porosity is then filled by liquid steel rich in oxygen, thus promoting further corrosion.

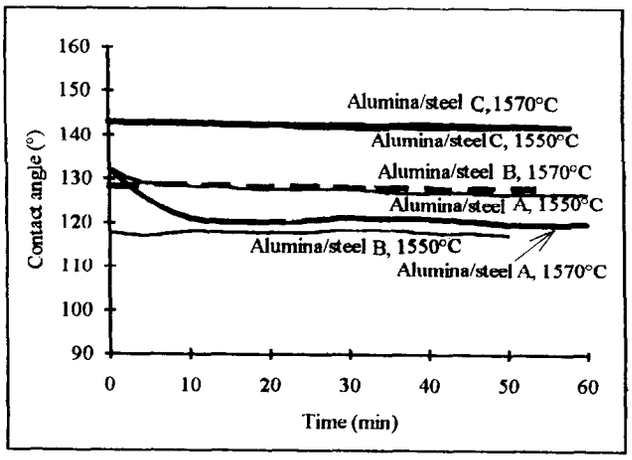

Fig. 7. θ evolution of steel/alumina contact.

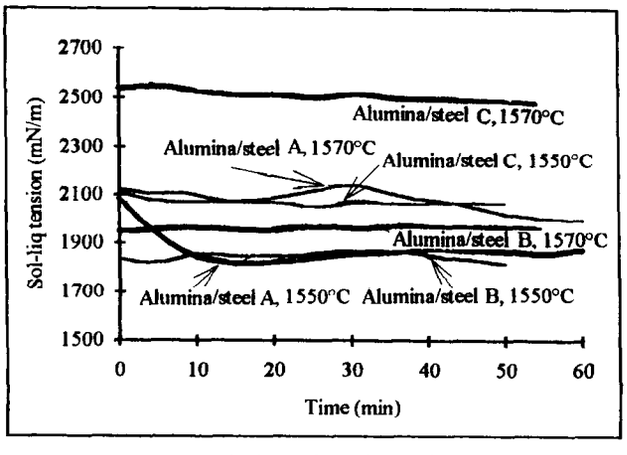

Fig. 8. σ_{SL} evolution of steel/alumina contact.

This type of behaviour is found in all types of steel studied with AlN. This effect was much more enhanced for steel B/AlN because of the presence of silicon which increases the wetting properties of the steel and forms silicon nitride as a result of a reaction with N_2 formed during the decomposition of AlN. This silicon nitride is again soluble in liquid steel[19] and this explains the fact that silicon is not detected at the interface. In the case of steel C, which is rich in titanium, nitrogen reacts with Ti to form TiN. This new phase is corrosion-resistant and helps in reducing or stopping corrosion wherever it forms. Thus we find that corrosion is almost constant at 0·16 mm in the case of steel C, during dipping experiments performed at 1550°C for 1 h.

Chemical interaction at liquid–vapour interface

A high concentration of aluminium and oxygen detected through EDAX shows that an alumina layer forms at the liquid drop surface. Thermodynamic calculations find the same results under our operating conditions. The wetting properties of a steel could then be related to this alumina layer formed at the surface, which keeps the angle of contact at a non-wetting value (Fig. 7) notably in the case of steel C. The speed of formation of this alumina layer depends on the type of steel, and can be rated as: C >> A ≥ B. In the case of steel C it appears 6 to 10 min after melting, and in the case of steel B, 40 min after fusion. Through thermodynamic calculations we find that in steel B, which is poor in aluminium, precipitation starts at 10 ppm of oxygen while it starts at 5 ppm in the case of steel C. This oxide layer has a strong influence on the wetting angle θ. The absence of AlON phase at the surface of samples having 20% porosity adds to the formation of this oxide layer and prevents real contact between steel and the AlN substrate, and thus corrosion is almost stopped (Table 4).

Conclusions

The modification of the contact angle between AlN and liquid steels is controlled by the degree of oxidation of AlN and of AlON present at grain boundaries through oxygen found in:

(1) the initial AlN powder, where it is present at about 1·5 wt%;
(2) the phases formed at the grain boundaries during the sintering of AlN;

(3) the furnace atmosphere where it is present at about 20 ppm, at a temperature between 1500 and 1600°C and at an argon pressure of about 10^5 Pa;
(4) steels, where its concentration varies from each type of steel C >> B ≈ A.

The mechanism of corrosion is complex: at the solid–liquid interface, corrosion takes place after AlN decomposition and alumina formation, and attacks the AlON phases present at grain boundaries. At the liquid–vapour interface, we detect the formation of an oxide layer (alumina) at the liquid drop surface.

For steel rich in Ti, we detect TiN at the solid–liquid interface. The formation of this phase is thermodynamically possible. TiN is corrosion-resistant and gives, where it forms, a higher corrosion resistance to AlN.

References

1. Vandemaele, Y., *Silicates Industriels*, **45**(12) (1980) 249.
2. Young, T., *Phil. Trans. Roy. Soc. London*, **95** (1805) 65.
3. Anerji, E. A., Rohatgi, P. K. & Reif, W., *Metall.*, **38** (1984) 656.
4. Gibbs, J. W., *Trans. Conn. Acad.*, **3** (1878) 343.
5. Johnson Jr., R. E., *J. Phys. Chem.*, **63** (1959) 1655.
6. Aksay, I. A., Hoge, C. E. & Pask, J. A., *J. Phys. Chem.*, **78**(12) (1974) 1178.
7. Delannay, F., Froyen, L. & Deruyttere, A., *J. Mater. Sci.*, **22** (1987) 1.
8. Labbe, J. C., Lachau-Durand, A., Laïmeche, A., Paulyou, V., Tétard, D. & Goujaud, J. F., *High Temp. Chem. Processes*, **1** (1992) 151.
9. Ado, G., Bernache, D. Billy, M., Hahn, K. S. & Lefort, P., *Rev. Chim. Mineral.*, **22** (1985) 473.
10. Wenzel, R., *Ind. Eng. Chem.*, **28** (1936) 988.
11. Rhee, S. K., *J. Am. Ceram. Soc.*, **54**(7) (1971) 334.
12. Coudurier, L., Pique, D. & Eustatopoulos, N., *J. Chim. Phys.*, **84** (1987) 2.
13. Marija, T. & Kolar, D., *J. Am. Ceram. Soc.*, **61** (1978) 5.
14. Sangiriogi, R., Muolo, M. L. & Passerone, A., *Mater. Sci. Monogr.*, **38A** (*High Tech. Ceram. Pt. A*) (1987) 415.
15. Laïmeche, A., Ph D Thesis, University of Limoges, 1993, p. 53.
16. Jones, L. M. & Nocholas, M. G., *J. Mater. Sci. Lett.*, **8** (1989) 265.
17. Billy, M., Jarrige, J., Lecompte, J. P., Mexmain, J. & Yefsah, S., *Rev. Chim. Mineral*, **19** (1982) 673.
18. Darbha, S., *J. Am. Ceram. Soc.*, **73** (4) (1990) 1108.
19. Yefsah, S., Billy, M., Jarrige, J. & Mexmain, J., *Rev. Int. Hautes Temp. Réfract., Fr.*, **18** (1981) 167.